

МЕЖЗВЕЗДНЫЕ ЛИНИИ В ОПТИЧЕСКИХ СПЕКТРАХ  
ВЫСОКОГО РАЗРЕШЕНИЯ CYG X-1 = V1357 CYGInterstellar Lines in High-Resolution Optical Spectra  
of Cyg X-1 = V1357 Cyg

**Резюме.** Исследовались узкие межзвёздные линии поглощения в оптических спектрах (3950 – 6690 Å) высокого разрешения ( $R = 75\,000$ ) Cyg X-1 = V1357 Cyg, полученных на 6-м телескопе САО РАН. Выявлены три основных абсорбционных компонента с гелиоцентрическими радиальными скоростями  $V_r = -1, -13$  и  $-22$  км/с, которые соответствуют трём газопылевым комплексам, расположенным на луче зрения до объекта. Это позволяет судить о распределении межзвёздного вещества на пути к Cyg X-1. В профилях наиболее сильных линий, возможно, присутствует слабый компонент с  $V_r = -45$  км/с, который мы связываем с расширяющейся межзвёздной оболочкой вокруг ассоциации Cyg OB3. Подтверждено, что Cyg X-1 образовался и до сих пор находится в этой ассоциации.

**Abstract.** High-resolution spectra ( $R = 75000$ ) of Cyg X-1 = V1357 Cyg obtained with the NES echelle spectrograph of the 6-meter telescope of SAO RAS (3950 – 6690 Å) were used for investigations of narrow interstellar absorption lines. The main three absorption components with heliocentric radial velocities  $V_r = -1, -13$  and  $-22$  km/s were revealed. They correspond to three interstellar gas-dust complexes on the line of sight toward the object. This allows us to determine the interstellar matter distribution on the way to Cyg X-1. In the profiles of the strongest lines a weak component with  $V_r = -40 \dots -50$  km/s is probably visible. We connect it with an expanding interstellar envelope around Cyg OB3 association. It is confirmed that Cyg X-1 was born and is up to now in this stellar association.

**Keywords.** Stars: X-ray binary: Cyg X-1 - Stars: V1357 Cyg - Stars: optical spectroscopy - ISM: interstellar lines - ISM: structure

## INTRODUCTION

Cyg X-1 is an X-ray binary system, whose relativistic component is the first black hole candidate. The optical component, an O9.7 Iab supergiant, is responsible for about 95% of the system's optical luminosity. But its absolute X-ray and optical luminosity values depend on the distance  $d$  to this X-ray binary. Recently it was determined ( $d = 1.8 - 2.0$  kpc) by using trigonometric radio parallax measurements (Reid et al. 2011). Earlier we supposed a somewhat larger distance ( $d = 2.0 - 2.3$  kpc) based on interstellar extinction measurements and Cyg X-1 location in the Cyg OB3 association, which lies at a distance of 2.3 kpc according to the old Galactic scale (Bochkarev & Karitskaya 2007). According to recent distance determination of OB-associations, Cyg OB3 is located at 1.8 kpc (Melnik & Dambis 2009). Thus,  $d = 1.8$  kpc for Cyg X-1 may be true.

An indirect test for what was said could be a determination of the number of interstellar complexes on the way toward Cyg X-1 and its comparison with independently observed

large-scale inhomogeneities of interstellar matter. For this purpose, this paper is devoted to an investigation of interstellar line profiles. We have used high-resolution spectra obtained on the 6-meter telescope in the framework of our program of long-term spectral monitoring of Cyg X-1 in the optical range (Karitskaya 2003; Karitskaya et al. 2006; Karitskaya et al. 2008).

## OBSERVATIONS

The observations were carried out with the NES echelle spectrograph of the 6-meter telescope of SAO RAS (North Caucasus). The detector was a CCD-camera ( $2k \times 2k$  pixels). During 20 nights in 2005–2008 68 spectra were obtained. The red region of the optical spectrum was observed in 2005 and 2008, and the blue one in 2006–2007 (Table 1). The spectral resolution is  $R \simeq 75,000$ . The signal-to-noise ratio  $S/N$  calculated per pixel in 1D-spectra is up to 330, which corresponds to  $\simeq 500$  per resolution element  $\simeq 4$  km/s.

Таблица 1: Table 1. Spectral observations of Cyg X-1 on the 6-meter telescope

Dates	$N_n^a$	$N_s^b$	Band, Å
12.11.2005	1	2	4557–6015
13–19.11.2005	2	6	5274–6693
14–15.03.2006	2	7	3978–5462
7–15.08.2006	6	24	4010–5460
24.07–5.09.2007	7	22	3943–5398
17–19.08.2008	2	7	4548–6005

**Notes:**  $a$  number of nights;  $b$  number of spectra.

## INTERSTELLAR LINES

The spectra reveal superstrong absorption lines of H I, He I, He II, blend CNO  $\lambda 4640$  Å, a lot of other lines of heavy elements (C, N, O, Ne, Mg, Si, S, Fe, Zn), and strong emission components of the H $\alpha$  and He II  $\lambda 4686$  Å lines with complicated and variable profiles. Also the spectra show narrow interstellar absorption lines as well as numerous diffuse interstellar bands (DIBs). In this paper we study only the profiles of narrow lines of atoms, of the CH molecule and of their ions (Table 2). For this purpose, all spectra were reduced to the heliocentric coordinate system and were added together. The resulting line profiles are shown in Figure 1.

The first column of Table 2 contains wavelengths of the measured interstellar lines. Wavelength  $\langle 4045 \rangle$  corresponds to the averaged profile of the weak doublet of K I 4044 and 4047 Å. It was smoothed by a Gaussian filter with a width of 2 km/s. The second column contains the species forming the lines. For the Ca II line and Na I doublet, Fraunhofer notations are also given. The third column gives the number of the averaged spectra. The fourth column gives the signal to noise ratio  $S/N$  calculated as square root of the number of counts in the summarized spectrum in the lines' neighbouring continuum. The fifth column shows the depth of the spectral lines relative to the continuum. The sixth column contains the radial velocity of the deepest part of the spectral lines. The next three columns give the linewidth in km/s at the levels 0.25, 0.5 and 0.75 of the line depth, respectively. The next to the last column gives the equivalent width of the line in mÅ. References to comments to rows of the table are in the last column.

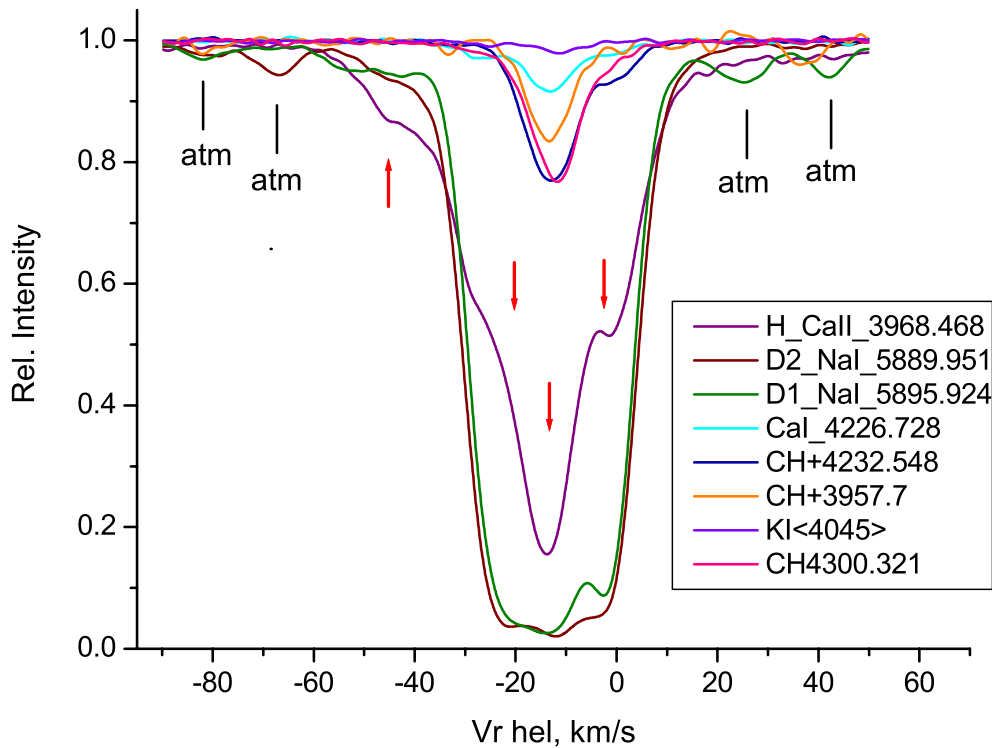


FIG. 1: Figure 1. Profiles of interstellar lines obtained from the 6-meter telescope Cyg X-1 optical spectra: relative intensity *vs* heliocentric radial velocity  $V_r$  *hel*. Profiles are shown by different colors according to the imbedded panel. Black ticks labeled “atm” mark positions of the terrestrial atmosphere  $H_2$  absorption lines on the D1 and D2 NaI line profiles. Red arrows indicate radial velocities of the main components of the interstellar line profiles.

Depressions seen in Figure 1 within spectrum fragments containing the D1 and D2 NaI line profiles marked by vertical black ticks are terrestrial atmospheric absorption lines of molecular hydrogen we have not omitted. Pollution with terrestrial lines occurs only in the red part of the spectrum, and within the shown spectrum fragments its depth does not exceed 5% of the relative intensity of the stellar continuum. Fortunately, the terrestrial lines overlapping with the interstellar absorption lines are weak enough and create distortion of their profiles not exceeding 2%. A weak terrestrial line occurs in the central part of D2 NaI line profile around  $V_r = -16$  km/s and distorts it by about 2%.

### STRUCTURE OF INTERSTELLAR MATTER TOWARD CYG X-1

In Figure 1, in the profiles of all strong enough interstellar lines one can see three main absorption components with heliocentric radial velocities  $V_r = -1$ ,  $-13$  and  $-22$  km/s, respectively. These components are considered as absorptions in interstellar gas-dust complexes on the line of sight toward the object. In addition, a weak component with  $V_r = -40 \dots -50$  km/s with a greater dispersion of velocities may be seen. On the figure the four components are marked with bold red arrows.

Таблица 2: Table 2. Measured interstellar lines in the Cyg X-1 optical spectra

Wavelength, Å	Species	$N_s^a$	$S/N$	Line depth	$V_r$ , km/s	$\Delta V_{0.25}$ , km/s	$\Delta V_{0.5}$ , km/s	$\Delta V_{0.75}$ , km/s	$W_\lambda$ , mÅ	Comm.
3957.7	CH <sup>+</sup>	22	150	0.166	−13.3	6.7	10.3	15.2	64	1
3968.468	H Ca II	22	170	0.843	−13.8	5.9	30.4	41.8	354	
4044.136	K I	53	200	0.027	−11.5	5	21	22	4.8	
4047.206	K I	53	200	0.014	−10.7	6	15	33	2.5	
<4045>	K I	53	250	0.021	−11.3	4.7	10	24	4.1	2
4226.728	Ca I	53	310	0.084	−13.1	7.2	11.4	30.4	21	
4232.548	CH <sup>+</sup>	53	290	0.230	−13.0	8.4	12.8	23.4	52	
4300.321	CH	53	330	0.233	−11.7	7.1	11.1	18.3	45	
5889.951	D2 Na I	15	240	0.980	−12.5	30.1	35.4	41	733	3
5995.924	D1 Na I	15	240	0.978	−14.4	28.8	33.5	38.7	691	3

**Notes:** <sup>a</sup>number of the spectra.

Comments: 1 – defect in the spectra, profile is not very reliable; 2 – summary profile of the K I doublet; 3 - profile is somewhat distorted because of overlapping weak terrestrial atmosphere line in parts of spectra marked in Figure 1 by black ticks.

It should be emphasized that the radial velocities in Table 2 and Figure 1 are heliocentric ones. To find the peculiar velocities of the gas clouds relative to local young Galactic objects (interstellar matter and massive stars) we should correct for the Sun’s peculiar velocity. Following Zabolotskikh et al. (2002) and Melnik & Dambis (2009), we adopted the value of the Sun’s peculiar velocity components in the Galactic coordinate system as  $u_0 = 10$  km/s,  $v_0 = 12 \pm 1$  km/s,  $w_0 = 7 \pm 1$  km/s. These three values do not depend on the adopted distance  $R_0$  to the center of the Galaxy, in fact at least for the  $R_0$  range 7.0–9.0 kpc (Melnik & Dambis, 2009). In this case, the peculiar velocity of the Sun toward Cyg X-1 is  $V_S = 15$  km/s. For the  $V_{\text{LSR}}$  velocities of the three main gas-dust complexes with respect to the Local Standard of Rest we get about +14 km/s, +2 km/s and −7 km/s respectively. These velocities are in a fair agreement with the Galactic rotation component toward Cyg X-1. For the fourth absorption line component  $V_{\text{LSR}} \approx -30$  km/s. The last component may be related generically to the Cyg 3 interstellar loop structure around the Cyg OB3 stellar association (Brand & Zealy, 1975; Bochkarev & Sitnik, 1985), on which the star Cyg X-1 is projected. In addition to equal distances to Cyg X-1 and Cyg OB3 ( $d = 1.8 - 2.0$  kpc, see Introduction), their proper motions coincide within the accuracy of the measurements. Indeed, for Cyg X-1 the proper motion as measured by Hipparcos is:  $\mu_\alpha = -0.00382 \pm 0.00079''$ ;  $\mu_\delta = -0.00762 \pm 0.00091''$ . According to Melnik & Dambis (2009), for Cyg OB3 the corresponding values are:  $\mu_\alpha = -0.0031 \pm 0.00025''$ ;  $\mu_\delta = -0.0071 \pm 0.00025''$ . The radial velocities are somewhat different: for Cyg X-1  $V_r = -3.3 \pm 1.1$  km/s (Aab, 1983),  $V_r = -2 \dots -11$  km/s (Abubekerev et al., 2004), and for Cyg OB3  $V_r = -9.5 \pm 1.8$  km/s (Melnik & Dambis, 2009). The difference is about 6 km/s, within the limits of the velocity dispersion for stars in Cyg OB3 association (9.5 km/s). Thus, most probably, Cyg OB3 is the place of Cyg X-1 birth and of its present location (Ziolkowski, 2005; Bochkarev & Kartiskaya, 2007). From the above values we estimate the upper limit on the kick-effect for the Cyg X-1 binary to be 16 km/s.

The 3D-distribution of obscuring interstellar dust in the region 2 kpc (in modern scale  $\simeq 1.6$  kpc) distance from the Sun constructed by Lucke (1978) with a resolution 200 pc indicates three matter condensations (gas-dust complexes) in the direction of Cyg X-1. The nearest (and the weakest) one is located at about 300 pc from the Sun. The second, the largest and most dense condensation is connected with the Great Rift dissecting the Milky Way from the constellation Cygnus to the galactic center and beyond. The edge of obscuring matter in the direction of Cyg X-1 closest to the Sun is at distance about 800 pc, the farthest edge being found at about 1300 pc (in the old galactic distance scale  $R_0 = 10$  kpc) and about 1 kpc in the modern one  $R_0 = 7 - 8$  kpc. The third gas-dust complex is located in Cygnus constellation star-formation region, connected with the associations Cyg OB1, Cyg OB2, Cyg OB3, and Cyg OB8 where Cyg X-1 is located. The nearest edge of the complex is at about 1.5 kpc (for modern  $R_0$ ).

With these three gas-dust complexes we connect the observed three components of the interstellar absorption line profiles (marked by arrows in Figure 1). The most powerful central component near the heliocentric radial velocity  $V_{r \text{ hel}} = -13$  km/s probably originates in the Great Rift. The other two are probably connected with the nearest and the farthest of the complexes. As the line of sight toward Cyg X-1 runs almost along the Local spiral arm,  $V_r$  is nearly constant along the way to this object:  $V_r$  variations are comparable with peculiar velocities of interstellar clouds as OB-associations (Melnik & Dambis 2009). Namely  $V_r$  in respect to local standard of rest are close to zero. It does not allow to tell which component is related to the farthest, and which to the nearest complex, although one can expect the line component with heliocentric velocity  $-1$  km/s ( $V_{\text{LSR}} = +14$  km/s) to be connected with the farthest gas-dust complex.

The interstellar absorption line profile components at heliocentric radial velocity  $-1$  km/s appear not only in the three strongest lines but also in the lines of CH<sup>+</sup> and Ca I. Line components at the radial velocity  $-20$  km/s appear in the same lines, but are a bit weaker. High velocity  $-45$  km/s components are detectable only in the strongest lines D1 and D2 Na I and H Ca II. It may indicate on differences of physical conditions and probably chemical composition in gas-dust complexes occurring on line sight.

## CONCLUSIONS

On the base of Cyg X-1 = V1357 Cyg high resolution spectra ( $R = 75,000$ ) obtained with the NES echelle spectrograph of the 6-meter telescope of SAO RAS, narrow interstellar absorption lines were studied. As a result of the investigation of interstellar line profiles, three main absorption components with heliocentric radial velocities  $V_r = -1, -13$  and  $-22$  km/s ( $V_{\text{LSR}} = +14$  km/s,  $+2$  km/s and  $-7$  km/s) were revealed.

These components were identified with interstellar gas-dust complexes on the line of sight toward Cyg X-1 up to its distance 1.8 kpc by comparing with the 3D-distribution of obscuring interstellar dust constructed by Lucke (1978). One of the dust complexes is located at about 300 pc from the Sun. The second, the largest and densest condensation producing the most powerful central absorption component is the Great Rift dissecting the Milky Way (located at distances 800 – 1300 pc). The rest one is produced in the Cygnus star-forming region containing Cyg OB associations, among them Cyg OB3, where Cyg X-1 is located ( $\geq 1500$  pc).

In addition, in the most strongest line profiles a weak component with  $V_r = -40 \dots -50$  km/s and a greater dispersion of velocities may be seen. It may be connected with the expanding interstellar envelope around the Cyg OB3 association.

Thus, the investigation of interstellar line profiles allows us to determine the interstellar matter distribution on the way toward Cyg X-1. The obtained pattern of this distribution is the extra argument in favor of the Cyg X-1 localization in the Cyg OB3 association at a distance of 1.8 kpc from the Sun. Other arguments are: coincidence of their localizations in the sky, proper motions, independently obtained distances. The difference in their radial velocities is found to be less than the velocity dispersion 9.5 km/s of the Cyg OB3 stars. Consequently, the X-ray binary Cyg X-1 was born in this association. The upper limit on the peculiar velocity acquired as a result of the SN explosion (kick-effect) for this object is about 16 km/s.

**Acknowledgements.** This study was supported by the Russian Foundation for Basic Research through grants 12-02-01237-a and 12-02-97006-a. We thank Prof. A.S. Rastorguev and A.M. Melnik for discussion.

## References

- Aab O.E., 1983, *Pis'ma v Azh*, **9**, 606  
 Abubekеров M.A., Antokhina E.A., Cherepashchuk A.M., 2004, *Astron. Rep.*, **48**, 550  
 Bochkarev N.G. & Sitnik T.G., 1985, *ApSS*, **108**, 237  
 Bochkarev N.G. & Karitskaya E.A., 2007, In: *Astrophysics and Cosmology after Gamow: Theory and Observations. Proceedings of the Gamow Memorial International Conference*. Eds.: G.S. Bisnovaty-Kogan et al., Cambridge (UK): Cambridge Scientific Publishers, 371  
 Brand P.W.J.L. & Zealey W.J. 1975, *A&A*, **38**, 363  
 Karitskaya E.A., 2003, *Kinematika i Fizika Nebesnykh Tel. Suppl. No. 4*, 230  
 Karitskaya E.A., Lyuty V.M., Bochkarev N.G., Shimanskii V. V., Tarasov A. E., Bondar A. V., Galazutdinov G. A., Lee B.-C., Metlova N.V., 2006, *Inf. Bull. Var. Stars*, No. 5678, 1  
 Karitskaya E.A., Bochkarev N.G., Bondar' A.V., Galazutdinov G.A., Musaev F.A., Sapar A.A., Shimanskii V.V., 2008, *Astron. Rep.*, **52**, 362  
 Melnik A.M. & Dambis A.K., 2009, *MNRAS*, **400**, 518  
 Reid M.J., McClintock J.E., Narayan R., et al. 2011, *ApJ*, **742**, 83  
 Zabolotskikh M.V., Rastorguev A.S., Dambis A.K., 2002, *Astron. Lett.*, **28**, 454  
 Ziolkowski J., 2005, *MNRAS*, **358**, 851

Sternberg Astron. Inst. of Lomonosov Moscow State University  
 13 Universitetskij prosp.  
 Moscow 119992, Russia  
 and Eurasian Astronomical Society,  
 13 Universitetskij prosp., Moscow 119992, Russia

Н.Г. Бочкарёв  
 N.G. Bochkarev  
*boch@sai.msu.ru*

Astronomical Institute of RAS,  
 48 Pyatnitskaya str.  
 Moscow. 119017 Russia

Е.А. Карицкая  
 E.A. Karitskaya

Special Astrophysical Observatory of RAS,  
 Nizhnij Arkhyz  
 369167, Russia

В.Г. Клочкова  
 V.G. Klochkova

Special Astrophysical Observatory of RAS,  
 Nizhnij Arkhyz  
 369167, Russia

М.В. Юшкин  
 M.V. Yushkin

Received February 23, 2013